Journal Pre-proofs

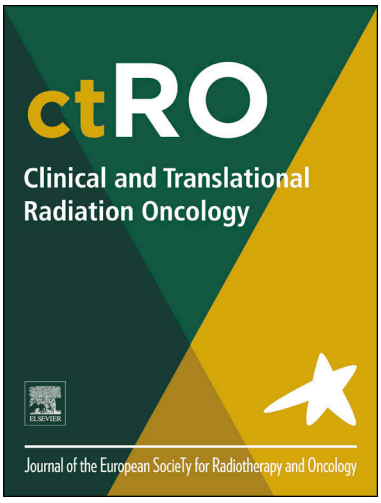

MRI-based radiomics to predict neoadjuvant chemoradiotherapy outcomes in locally advanced rectal cancer: A multicenter study

Yirong Xiang, Shuai Li, Hongzhi Wang, Maxiaowei Song, Ke Hu, Fengwei Wang, Zhi Wang, Zhiyong Niu, Jin Liu, Yong Cai, Yongheng Li, Xianggao Zhu, Jianhao Geng, Yangzi Zhang, Huajing Teng, Weihu Wang

PII: S2405-6308(22)00108-2
DOI: https://doi.org/10.1016/j.ctro.2022.11.009
Reference: CTRO 550

To appear in: *Clinical & Translational Radiation Oncology*

Received Date: 10 October 2022
Revised Date: 12 November 2022
Accepted Date: 14 November 2022

Please cite this article as: Y. Xiang, S. Li, H. Wang, M. Song, K. Hu, F. Wang, Z. Wang, Z. Niu, J. Liu, Y. Cai, Y. Li, X. Zhu, J. Geng, Y. Zhang, H. Teng, W. Wang, MRI-based radiomics to predict neoadjuvant chemoradiotherapy outcomes in locally advanced rectal cancer: A multicenter study, *Clinical & Translational Radiation Oncology* (2022), doi: https://doi.org/10.1016/j.ctro.2022.11.009

MRI-based radiomics to predict neoadjuvant chemoradiotherapy outcomes in locally advanced rectal cancer: A multicenter study

Yirong Xiang [1*], Shuai Li [1*], Hongzhi Wang [1*], Maxiaowei Song [1], Ke Hu [2], Fengwei Wang [3], Zhi Wang [4], Zhiyong Niu [4], Jin Liu [4], Yong Cai [1], Yongheng Li [1], Xianggao Zhu, MD [1], Jianhao Geng [1], Yangzi Zhang [1], Huajing Teng [1#], Weihu Wang [1#]

[1]Key Laboratory of Carcinogenesis and Translational Research (Ministry of Education/Beijing), Department of Radiation Oncology, Peking University Cancer Hospital and Institute

[2]Department of Radiation Oncology, Peking Union Medical College Hospital, Chinese Academy of Medical Sciences & Peking Union Medical College

[3]Department of Oncology, Tianjin Union Medical Center

[4]Blot Info & Tech (Beijing) Co. Ltd

[*] Yirong Xiang, Shai Li and Hongzhi Wang contributed equally to this work.

[#] Correspondence to:

Weihu Wang

Key Laboratory of Carcinogenesis and Translational Research (Ministry of Education/Beijing), Department of Radiation Oncology, Peking University Cancer Hospital and Institute, Beijing 100142, China, E-mail: wangweihu88@163.com

Huajing Teng

Key Laboratory of Carcinogenesis and Translational Research (Ministry of Education/Beijing), Department of Radiation Oncology, Peking University Cancer Hospital and Institute, Beijing, China. E-mail: hjteng@bjmu.edu.cn

Abstract

Background and purpose: Predicting tumour response would be useful for selecting patients with locally advanced rectal cancer (LARC) for organ preservation strategies. We aimed to develop and validate a prediction model for T downstaging (ypT0-2) in LARC patients after neoadjuvant chemoradiotherapy and to identify those who may benefit from consolidation chemotherapy.

Materials and methods: cT3-4 LARC patients at three tertiary medical centers from January 2012 to January 2019 were retrospectively included, while a prospective cohort was recruited from June 2021 to March 2022. Eight filter (principal component analysis, least absolute shrinkage and selection operator, partial least-squares discriminant analysis, random forest)-classifier (support vector machine, logistic regression) models were established to select radiomic features. A nomogram combining radiomics and significant clinical features was developed and validated by calibration curve and decision curve analysis. Interaction test was conducted to investigate the consolidation chemotherapy benefits.

Results: A total of 634 patients were included (426 in training cohort, 174 in testing cohort and 34 in prospective cohort). A radiomic prediction model using partial least-squares discriminant analysis and a support vector machine showed the best performance (AUC: 0.832 [training]; 0.763 [testing]). A nomogram combining radiomics and clinical features showed significantly better prognostic performance (AUC: 0.842 [training]; 0.809 [testing]) than the radiomic model. The model was also tested in the prospective cohort with AUC 0.727. High-probability group (score>81.82) may have potential benefits from ≥4 cycles consolidation chemotherapy (OR: 4.173, 95% CI: 0.953–18.276, p = 0.058, $p_{interaction}$ = 0.021).

Conclusion: We identified and validated a model based on multicenter pre-treatment radiomics to predict ypT0-2 in cT3-4 LARC patients, which may facilitate individualised treatment decision-making for organ-preservation strategies and consolidation chemotherapy.

Keywords: rectal cancer, radiomics, neoadjuvant treatment

Abbreviations

AUC, area under the curve
DA, discriminant analysis
CEA, Carcinoembryonic antigen
FOLFOX, fluorouracil plus oxaliplatin
IDI, integrated discrimination improvement
LARC, locally advanced rectal cancer
LASSO, least absolute shrinkage and selection operator
MRI, magnetic resonance imaging
NRI, net reclassification improvement
PCA, principal component analysis
PLS, partial least squares
RF, random forest
ROC, receiver operating characteristic
ROI, region-of-interest
SVM, support vector machine
T2WI, T2-weighted imaging
TEM, endoscopic microsurgery
TME, total mesorectal excision
XELOX, capecitabine plus oxaliplatin

1. Introduction

Neoadjuvant treatment followed by total mesorectal excision (TME) is the standard treatment for locally advanced rectal cancer (LARC) (1). However, TME is associated with a high risk of perioperative morbidity, temporary or permanent functional impairment, and a decreased quality of life (2, 3). Local resection, such as transanal endoscopic microsurgery (TEM), is an organ-preserving treatment option associated with a shorter operative duration and fewer perioperative complications (4, 5). Nevertheless, a high local recurrence rate limits TEM application to patients with LARC, indicating the need to carefully select eligible patients (6). Neoadjuvant treatment use induces tumour downstaging and reduces local recurrence risk, which is expected to expand TEM use to patients with advanced LARC (7-9). Patients with a complete or "near" complete response to neoadjuvant treatment followed by TEM could achieve good oncological outcomes and improved quality of life (7, 10). Therefore, a means to predict tumour response and pathological downstaging could facilitate the selection of patients with LARC who could potentially benefit from organ preservation.

Recently, several trials have aroused interest in implementing consolidation chemotherapy between concurrent chemoradiotherapy and surgery in patients with LARC to improve tumour regression (11, 12). Additionally, compared to adjuvant chemotherapy, upfront consolidation chemotherapy may promote treatment adherence and tolerance. However, there is no consensus on its long-term benefits; the precise regimen for consolidation chemotherapy remains unclear (13). Thus, it is important to accurately select patients who would benefit more from this approach and investigate appropriate treatment strategies.

Magnetic resonance imaging (MRI) has been widely used to inform clinical diagnosis and staging and for quantitatively predicting prognosis in patients with rectal cancer (14). Using high-throughput extraction of imaging information invisible to the eye, and converting it into quantitative features, radiomics can effectively improve diagnostic accuracy, evaluate treatment response, and predict survival prognosis (15-17). Herein, we aimed to develop and validate a prediction model combining radiomic and clinical features for T downstaging (ypT0-2, AJCC 8th) in patients with cT3-4 LARC following neoadjuvant treatment. Using the model, we tried to identify patients who may benefit from consolidation chemotherapy and investigated appropriate treatment strategies.

2. *Material and Methods*

2.1 Patients and treatment

This multicenter study was approved by the ethics committee of Beijing Cancer Hospital (2018KT78), and the requirement for obtaining informed patient consent was waived. The registration number for prospective design is ChiCTR2100048015.

We respectively recruited patients with LARC between January 2012 and January 2019 at three different centres who 1) had histologically confirmed adenocarcinoma; 2) were MRI-confirmed cT3-4 (AJCC 8th), and 3) underwent standard concurrent chemoradiotherapy with or without consolidation chemotherapy followed by TME. Patients were excluded if they 1) were <18-year-old, 2) had an Eastern Cooperative Oncology Group score >1, or 3) MRI images (T2-weighted imaging, T2WI) before neoadjuvant treatment were not available; 4) had metastases at baseline. Consequently, 600 patients were included and were randomly divided, at a 7:3 ratio, into training (n=426) and testing (n=174) cohorts. Using the same inclusion and exclusion criteria, a prospective cohort was recruited from June 2021 at centre 1 (n=34). Consequently, we included a training cohort, an internal validation cohort (testing cohort), and a prospective validation cohort (prospective cohort).

Baseline characteristics, including demographic information, clinicopathologic evaluations, and T2W images before neoadjuvant treatment, were collected from medical records. Neoadjuvant treatment included concurrent chemoradiotherapy with or without consolidation chemotherapy. The concurrent chemoradiotherapy strategy was long-course chemoradiotherapy (22–25 fractions of 2–2.3 Gy for primary rectal tumours, and 1.8–2 Gy for planning target volume, which contained the mesorectal area and internal iliac, obturator, and presacral lymphatic drainage area) with capecitabine 825 mg/m^2 (18). The consolidation chemotherapy was a fluorouracil-based regimen, either oral capecitabine, fluorouracil plus oxaliplatin (FOLFOX), or capecitabine plus oxaliplatin (XELOX). All patients underwent radical surgery based on TME principles.

2.2 MRI protocol and imaging feature extraction

Patients were scanned with 3.0-T MRI (Siemens Magnetom Skyra; GE Signa HDX; or GE OPTIMA) within 2 weeks prior to neoadjuvant treatment. No bowel preparation was required pre-examination. Each patient's MRI image was exported and collated in Digital Imaging and Communications in Medicine format.

Four board-certified radiation oncologists with >5 years' experience independently and manually delineated the region-of-interest (ROI) for primary rectal tumours on T2W images. Then, a radiation expert with 20 years' experience verified tumour masking. All images were standardised using Z-scores to minimize image intensity variations. 3D reconstruction was conducted using the Marching Cube algorithm with a 1×1×1-mm voxel. Eventually, 786 imaging features, including 42 texture features, 48 wavelet features, 540 histograms of oriented gradient features, and 156 statistical features, were extracted.

2.3 Feature selection and radiomic signature construction

To remove invalid information and avoid overfitting, we excluded the features quantified as infinite or null and features with extremely small variances. We then calculated the Pearson correlation coefficients for each radiomic feature pair. For those with r>0.9, we removed those with larger mean absolute correlations. We subsequently ranked the features by Pearson correlation coefficients for the outcome and selected the top-20% features. Consequently, 87 radiomic features were selected for further screening. To identify the most useful prognostic features for the radiomic predictive model, eight filter–classifier algorithms were used, including principal component analysis (PCA) and support vector machine (SVM), PCA and logistic regression (LR), least absolute shrinkage and selection operator (LASSO) and SVM, LASSO and LR, partial least-squares discriminant analysis (PLS-DA) and (SVM), PLS-DA and LR, random forest (RF) and (SVM), and RF and LR. PLS is called a "supervised" version of PCA. By constructing the linear combinations of the explanatory variables (to the corresponding dependent variable, ypT0-2), high-dimensional radiomic features could be filtered to fewer components, permitting prediction of the corresponding outcome (ypT0-2) (17, 19). Hyperparameters were selected, thus eight prediction models were built in the training cohort and validated in the testing cohort. Finally, the model with the best performance and stabilisation in both cohorts was selected to establish a radiomic prediction model, by which we calculated radiomic scores.

2.4 Prediction model development and validation

Univariate and multivariate LR analyses were used to determine the clinical features associated with ypT0-2. Pearson correlation analysis was conducted to explore the correlations between each clinical features pair. Then, three prediction models, including a clinical model (consisting of clinical features), a radiomic model (as mentioned above), and a radiomic-clinical model (combining clinical scores and radiomic scores),

were constructed. The predictive performance of each model in the training and testing cohorts was assessed using a calibration curve and receiver operating characteristic (ROC) curve analysis, in which the areas under the curves (AUCs) were reported (95% CIs calculated by bootstrap method). Furthermore, prognostic differences were quantified by net reclassification improvement (NRI) and integrated discrimination improvement (IDI) values. A radiomic-clinical nomogram was established. The nomogram was further validated in our prospective cohort using ROC curve. The Schematic overview of the proposed approach for "*Feature selection and radiomic signature construction"* and *"Prediction model development and validation*" part is shown in eFigure 1.

2.5 Patient stratification and consolidation chemotherapy efficacy

The threshold for a high and a low probability of achieving T downstaging was determined by ROC curve analysis, and the net benefit of this threshold probability was evaluated by decision curve analysis (DCA). Patients were stratified into high- (good responders) and low- (poor responders) probability groups. To identify patients who may benefit from consolidation chemotherapy, stratified analyses and p-interaction tests were performed.

2.6 Statistical analysis

The primary outcome was histological T downstaging (ypT0-2) from initial cT3-4, which was determined post-surgery using pathological slices. Continuous variables are presented as median along with interquartile range, and were compared using the Mann–Whitney U test. Categorical variables were compared between groups using the Chi-Square test or Fisher's exact test, as appropriate. Differences were considered statistically significant at $p<0.05$. Univariate analyses, multivariate analyses and interaction test were performed using SPSS v. 23.0 software (IBM SPSS Corp., Armonk, NY, USA). The MRI Dicom images were uploaded to and standardised in Precision Medicine Open Platform version 2.0.1 (https://www.blothealth.com). Using this software, we delineated ROIs and extracted radiomics features (20, 21). Feature selection and model construction were conducted using R software (version 4.0.5; https://www.r-project.org). The packages used included glmnet, caret, e1071, pROC, VIM, foreign, rms, randomForest, PredictABEL, riskRegression, rmda, and nomogramFormula. PLS-DA was performed using SIMCA software (v. 14.1; https://www.sartorius.com/en/products/process-analytical-technology/data-

analytics-software/mvda-software/simca).

3. Results

3.1 Patients characteristics

Six hundred patients were included in the study. Table 1 shows the clinicopathological characteristics of the patients in the training and testing cohorts. No significant differences were observed between the cohorts. The baseline characteristics for prospective cohort was shown in eTable 1. Altogether, 258/426 (60.6%), 95/174 (54.6%), and 23/34 (67.6%) achieved the primary outcome (ypT0-2) for training cohort, internal testing cohort, and prospective testing cohort (Chi-square test, p=0.189), respectively.

Table 1 Demographic and clinical characteristics.

	Training cohort (n = 426)		Testing cohort (n = 174)		p value
	n/median	%/IQR	n/median	%/IQR	
Age (years)	58	50, 65	58	48, 64	0.361
Sex					
Female	116	27.23	59	33.91	0.102
Male	310	72.77	115	66.09	
Centre					
1	169	39.67	78	44.83	0.487
2	116	27.23	45	25.86	
3	141	33.10	51	29.31	
CEA					
≥ 5ng/ml	257	60.33	101	58.05	0.605
< 5ng/ml	169	39.67	73	41.95	
Pathological differentiation					
High	64	15.02	20	11.49	0.391
Moderate	248	58.22	114	65.52	
Poor	23	5.40	7	4.02	
Location: distance from anus					
< 5 cm	183	42.96	79	45.40	0.259
5–10 cm	238	55.87	90	51.72	
>10 cm	5	1.17	5	2.87	
Clinical T stage					
T3	331	77.70	130	74.71	0.431
T4	95	22.30	44	25.29	
Consolidation chemotherapy					
Not done	307	72.07	126	72.41	0.881
0–3 cycles	84	19.72	32	18.39	
4 cycles	35	8.22	16	9.20	
Pathological T stage					

0	114	26.76	44	25.29	0.554
1	31	7.28	10	5.75	
2	113	26.53	41	23.56	
3	162	38.03	76	43.68	
4	6	1.41	3	1.72	
Pathological N stage					
0	332	77.93	120	68.97	0.106
1	70	16.43	38	21.84	
2	24	5.63	16	9.20	
ypT0N0					
yes	104		40		0.711
no	332		134		

IQR: interquartile range; CEA, Carcinoembryonic antigen. Continuous variables are presented as median along with interquartile range, and were compared using the Mann–Whitney U test. Categorical variables were compared between groups using the Chi-Square test or Fisher's exact test, as appropriate. Differences were considered statistically significant at $p<0.05$.

3.2 Radiomic signature construction

The prediction performance of the eight feature-selection strategies and classifier groups are shown in Table 2. Among the eight groups, PLS-DA-SVM had high AUCs in both the training (AUC=0.832) and testing (AUC=0.763) cohorts. Using PLS-DA, the radiomic features were dimensionally reduced to four components, without overfitting. Detailed information of radiomic signatures selection is presented in eFigures 2 and eTable 2–3. We thus built a radiomic prediction model and calculated the radiomic scores from PLS-DA-SVM.

Table 2. Diagnostic performances of different models

AUC	PCA-SVM	PCA-LR	LASSO-SVM	LASSO-LR
Training cohort	0.818	0.796	0.824	0.825
Testing cohort	0.752	0.74	0.755	0.765
AUC	PLS-DA-SVM	PLS-DA-LR	RF-SVM	RF-LR
Training cohort	0.832	0.829	0.821	0.813
Testing cohort	0.763	0.761	0.722	0.742

AUC: area under the curve; PCA-SVM: principal component analysis and support vector machine; PCA-LR: principal component analysis and logistic regression; LASSO-SVM: least absolute shrinkage and selection operator and support vector machine; LASSO-LR: least absolute shrinkage and logistic regression; PLS-DA-SVM: partial least-squares discriminant analysis and support vector machine; PLS-DA-LR: partial least-squares discriminant analysis and logistic regression; RF-SVM: random forest and support vector machine; RF-LR: random forest and logistic regression.

3.3 Comprehensive prediction model development

Based on the clinical background and multivariate regression analysis (eTable 4, eFigure 3), we included clinical T stage, serum CEA level, and tumour location as clinical predictors to build the clinical prediction model with the corresponding score. Therefore, three prediction models were established: a clinical model (built upon clinical predictors), a radiomic model (built upon PLS-DA-SVM), and a radiomic-clinical model (built upon clinical and radiomic scores). The calibration curves for these 3 models (Figure 1A, D) showed good agreement between the predicted risk and actual frequency. Figures 1B and E showed that the radiomic-clinical model provided the best predictive performance in the training (AUC 0.842, 95% CI 0.806–0.880) and testing cohorts (AUC 0.809, 95%CI 0.744–0.873). Additionally, the combined model achieved a significant reclassification improvement, as measured by NRI and IDI (eTable 5). A nomogram was constructed using the radiomic-clinical prediction model in the training cohort (Figure 2). The threshold for classifying high (good responders) and low probability (poor responders) of achieving pathological T downstaging was calculated by Youden's statistic (sensitivity + specificity - 1=0.635) from the ROC curve, which corresponded to 81.82 points in the nomogram. The decision curve presented in Figures 1C and F reveals that this cut-off probability yielded net clinical benefits in both cohorts. The nomogram was additionally validated in the prospective cohort with AUC 0.727 (ROC curve shown in eFigure 4).

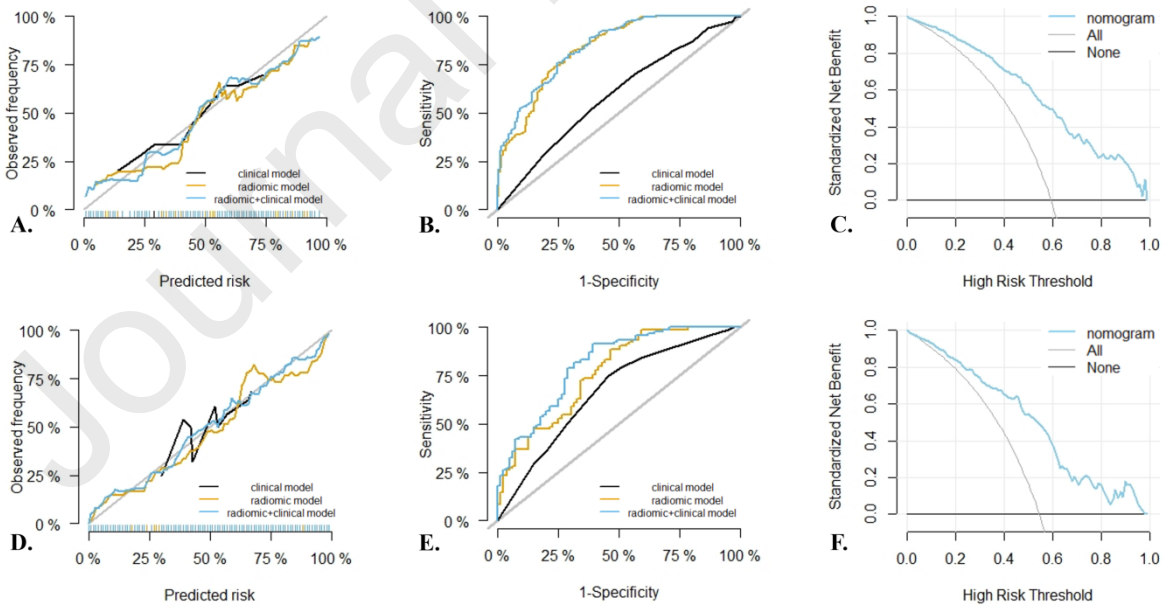

Figure 1. Calibration curves, receiver operating characteristic (ROC) curves and decision curves of the models for predicting pathological T downstaging. (A–C) The calibration curves, ROC curves, and decision curves in the training cohort, respectively. (D–F). The calibration curves, ROC curves, and decision curves in the testing cohort.

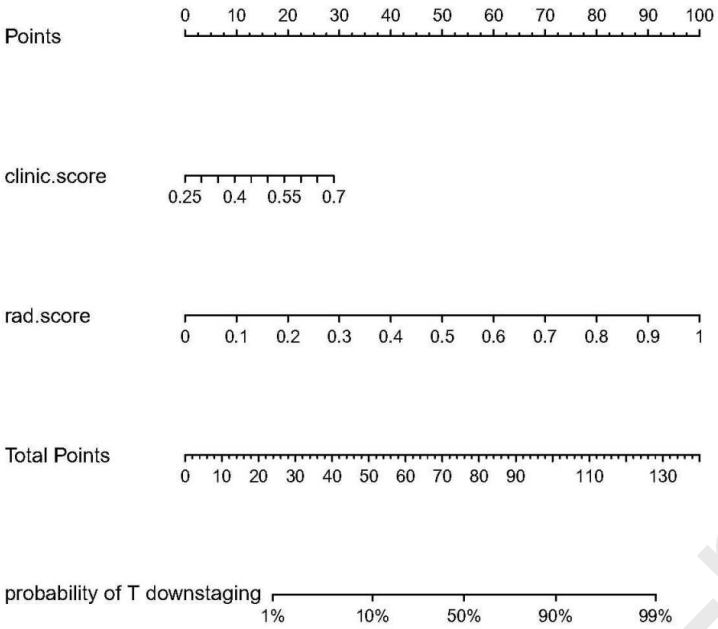

Figure 2. The nomogram combining radiomics and clinical features. Clinic. score is defined as logistic regression probability for ypT0-2 by clinical variables including clinical T stage, serum CEA level, and tumor location. Rad. score is defined as predictive probability for ypT0-2 by radiomic prediction model.

3.4 Consolidation chemotherapy efficacy exploration

To select appropriate patients eligible for consolidation chemotherapy, we performed an interaction test between tumour response to pT downstaging and consolidation chemotherapy efficacy. Compared to patients who did not receive consolidation chemotherapy, patients who received any cycles of consolidation chemotherapy obtained no benefits from the treatment (Table 3). However, p-interaction analysis revealed that among poor responders and good responders to concurrent chemoradiotherapy therapy, ≥4 cycles of consolidation chemotherapy showed different efficacy ($p_{interaction}$=0.021). Good responders (High-probability group) may have potential benefits from ≥4 cycles of consolidation chemotherapy (OR 4.173, 95% CI 0.953–18.276, p=0.058).

Table 3. Treatment interaction with nomogram risk stratification for pathologic T downstaging

Consolidation Chemotherapy	Not done (n=433)		Done (n=167)		Crude		p for interaction	Adjusted		p for interaction
	Total	pT0-2 (%)	Total	pT0-2 (%)	OR (95%CI)	p		OR (95%CI)	p	
Poor responders	195	61 (31.3%)	75	26 (36.7%)	1.166 (0.663, 2.048)	0.594	0.733	1.177 (0.663, 2.088)	0.578	0.454
Good responders	238	190 (79.8%)	92	71 (77.2%)	0.854 (0.478, 1.527)	0.595		0.836 (0.464, 1.515)	0.555	
	0-3 cycles (n=549)		≥4 cycles (n=51)		Crude		P for interaction	Adjusted		P for interaction
	Total	pT0-2 (%)	Total	pT0-2 (%)	OR (95%CI)	p		OR (95%CI)	p	
Poor responders	248	83 (33.5%)	22	4 (18.2%)	0.442 (0.145, 1.347)	0.151	0.021	0.438 (0.141, 1.360)	0.153	0.021
Good responders	301	234 (77.7%)	29	27 (93.1%)	3.865 (0.896, 16.674)	0.070		4.173 (0.953, 18.276)	0.058	

OR: odds ratio; CI: confidence interval.

4. Discussion

In this multicentre cohort, we focused on using pre-treatment T2WI-based radiomics to predict outcomes in patients with cT3-4 LARC who underwent neoadjuvant treatment in terms of downstaging to ypT0-2. A nomogram combining radiomic features and clinical information was constructed and showed prognostic abilities with AUC 0.842 (training), 0.809 (testing), and 0.727 (prospective). The prediction model was validated using a calibration curve, and the clinical utility was verified by DCA. Consolidation chemotherapy for ≥4 cycles may improve the T downstaging rates in good responders rather than poor responders.

The standard treatment for patients with LARC is neoadjuvant treatment followed by TME. However, surgical resection has been associated with significant rates of stoma construction, morbidity, and mortality (22). Therefore, organ-preserving strategies, such as local surgery (e.g., TEM), which involves minimal morbidity and mortality and short postoperative recovery, have gained interest in recent years (23). With widespread neoadjuvant treatment use, 15–27% of patients achieve a pathological complete response (pCR), and 60–70% reach tumour downstaging after neoadjuvant treatment (24-26). Following neoadjuvant treatment, TEM may play an extended role in carefully selected patients with LARC for active surveillance (8, 9). Rutger *et al*. recruited 47 patients with MRI-confirmed cT1-3N0-1M0 LARC, and revealed that, after neoadjuvant treatment followed by TEM, the 5-year local recurrence rate, 5-year disease-free and overall survival rates were 7.7%, 81.6%, and 82.8%, respectively (7). Creavin *et al*. found that, in patients with cT1-4N0-2M0 LARC and an objective response to neoadjuvant treatment (residual scar/ulcer ≤3 cm), similar oncological outcomes were achieved between the organ-preservation strategy and TME (6). Therefore, we speculated that a broad range of patients with LARC might benefit from organ-preservation strategies with sufficient neoadjuvant treatment. Herein, we chose ypT0-2 as the endpoint, as we sought to select appropriate patients with LARC for organ preservation. Moreover, we chose ypT0-2 rather than pCR, which is the usual surrogate endpoint, as the primary outcome is because the pCR rate does not correspond with outcomes in patients who did not achieve pCR (only 15–27% of patients achieved pCR). Additionally, the low-risk subgroup (ypStageI) had long-term oncological outcomes similar to those of its pCR counterpart (27). Additionally, several clinical trials focused on extending organ-preservation strategies to more advanced patients (shown in eTable 6). Pooled analysis showed that there was non-significant for local excision and radical surgery in 5-year DFS and 10-year OS in patients with stage cT1-4NxM0 before neoadjuvant

treatment (28). Sajid et al included 10 trials and 942 cT1-2NxM0 patients with or without neoadjuvant chemoradiotherapy. They reported a higher risk of local recurrence (OR 2,78, p<0.003) but similar overall survival (OR 0.90, p=0.74) for TEM compared with radical resection (4). With rapidly developing local excision surgery strategies, including trans-anal minimally invasive surgery (TAMIS) and pyramid excision (29, 30), intensive neoadjuvant treatment, high selection for appropriate patients, and close follow-ups (31-34), we think more patients could benefit from organ-preservation strategies. Consequently, we chose ypT0-2 as the primary outcome.

In terms of pathologic lymph node metastasis, we included ypT0-2NanyM0 instead of ypT0-2N0M0 as the primary outcome. Previous studies demonstrated that MRI-based radiomics could be a potential marker for predicting lymph node status after neoadjuvant treatment; however, most of these studies used images from post-neoadjuvant treatment or from both pre- and post-neoadjuvant treatment (35-38). It remains unknown whether only the usage of pre-neoadjuvant treatment MR images can precisely predict the pN stage. Moreover, in the GRECCAR-2 trial, pathological N+ in ypT2 patients who received local excision was low (2/28, 7.1%) (33). Herein, we included cT3-4 patients, and most of our ypT0-2 patients had negative pathological lymph nodes (301/348, 86.5%). Third, Ma *et al.* selected 11 radiomic features and used the RF method to establish a predictive model for pathological N stage. They selected different radiomic features and used different model construction methods (multilayer perceptron) to build a predictive model for pathological T stage. It is supposed that to predict pathological T or N stages, respectively, we should use different radiomic features and diverse model construction methods (39). Adding pathological N stage to the primary outcome might reduce predictive effect reliability on pT stage. We speculated that, to predict ypN0, the region of positive lymph nodes should be delineated in the ROI and clinicopathological features, including ypT stage and cN stage before neoadjuvant treatment (40-42), which predict ypN0, should be included.

MRI-based radiomics has attracted attention for rectal cancer treatment and can be used to reveal tumour heterogeneity, which is difficult to identify: e.g., positive circumferential resection margin (43), preoperative synchronous distant metastasis (44), or pathological stages (39). MRI-based radiomics is associated with treatment response and long-term prognosis (15-17, 45). Most previous MRI-based radiomic studies used pCR as a short-term outcome for neoadjuvant therapy response. Bulens *et al*. developed a post-neoadjuvant treatment MRI-based prediction model for pCR with AUCs of 0.86 (95%CI 0.75–0.98) and 0.86 (95% CI

0.76–0.97) in the development (n=70) and external validation cohort (n=55), respectively (16). Liu *et al*. established a pre- and post-neoadjuvant treatment MRI-based radiomics model to predict pCR (AUC 0.976, 95% CI 0.919–0.971) in 222 patients with LARC (46). Wan *et al*. used a radiomic model combining T2WI and diffusion-weighted imaging delta sequences and achieved AUCs of 0.91 (95% CI 0.85–0.98) and 0.91 (95% CI 0.83–0.99) in the training and testing sets, respectively. A single-centre study enrolled 383 patients with LARC and constructed a pre- and post-neoadjuvant treatment MRI-based radiomics prediction model for pCR with an AUC of 0.99 (95% CI 0.98–1.00) and T downstaging (pT0-2) with an AUC of 0.79 (95% CI 0.69–9.87) (47). These studies proved the value of MRI-based radiomics for predicting tumour response to neoadjuvant treatment. Additionally, radiomic signatures were shown to be related to adjuvant chemotherapy benefits for distant control in patients with LARC (15). Recently, a new radiomic approach named delta radiomics has been developed. It extracts the key variations of radiomic features from images in different time-points. In rectal cancer, delta radiomics was utilized in predicting oncological outcomes such as TRG status, pCR, cCR and distant metastasis (48-53). Here, PLS-DA was used for radiomic features selection; the radiomics signature showed considerable predictive power (AUC: 0.832 [training], 0.763 [testing]). As for clinical features, based on multivariate regression and previous studies and clinical background, we chose pre-treatment CEA (multivariate regression p=0.003, (54, 55)), clinical tumour stage (multivariate regression p=0.005, (56, 57)) and tumour location (58, 59). We established a combined prediction nomogram based on MRI-radiomics and clinical features with AUC 0.842 for the training cohort and 0.809 for the testing cohort, respectively. Additionally, we validated the model in a prospective cohort with AUC 0.727, which primarily indicated its robustness and reliability.

Stratification by the radiomic-clinical nomogram showed that patients with good responders (here high-probability signatures) benefited from adequate consolidation chemotherapy. Previous studies failed to reach a consensus regarding the consolidation chemotherapy efficacy. The CAO-12 study revealed that concurrent chemoradiotherapy followed by consolidation chemotherapy may result in better pCR rates than those with pre-concurrent chemoradiotherapy induction chemotherapy (12). Garcia *et al*. performed a prospective, non-randomised, multicentre phase II study (Timing study) with 259 patients with LARC treated with long-course concurrent chemoradiotherapy. Compared with 18% in patients without consolidation chemotherapy, the pCR rate increased to 25%, 30%, and 38% by adding 2, 4, and 6 cycles of FOLFOX6 consolidation chemotherapy, respectively (p=0.0036) (11). However, in the randomised WAIT trial, pCR rates between

patients with and without 3 cycles of fluorouracil-based consolidation chemotherapy after standard concurrent chemoradiotherapy therapy were similar (16% vs. 25%, p=0.49) (60). Therefore, it is unclear for whom consolidation chemotherapy should be provided and when. We stratified patients using the predictive nomogram. Any number of consolidation chemotherapy cycles showed no benefits in either poor or good responders. However, good responders and poor responders showed different responses to ≥4 cycles consolidation chemotherapy ($p_{interaction}$=0.021). Consolidation chemotherapy for ≥4 cycles may improve T downstaging rates in good responders in the edge of significance (OR 4.173, 95% CI 0.953–18.276, p=0.058). It is indicated that those with high probabilities of achieving good treatment responses might be potentially selected for adequate consolidation chemotherapy. Consequently, the model can be a useful tool in clinical practice to predict the response to neoadjuvant treatment and to personalize treatment strategies of organ-preservation surgery and consolidation chemotherapy.

Our prediction model has the advantage of using several statistical methods for radiomic feature selection and model construction. This procedure guaranteed that the more important features were filtered, and the model with better performance was established. Furthermore, PLS-DA is highly effective in avoiding overfitting and identifying important features for dependent outcome prediction, particularly in omics fields, where the sample sizes are significantly smaller than the number of features (19). In rectal cancer, Delli *et al*. (17) used PLS regression to construct an MRI-based clinical-radiomics prediction model for major pathological treatment response (AUC 0.793, p<0.001). Our PLS-DA showed good predictive performance with both SVM and LR modelling methods, indicating its potential advantages in radiomics research. Another advantage of the model is that we included 600 patients from three different centres and randomly assigned them to training and testing cohorts; we recruited a prospective cohort to further assess the model. Thus, the large sample size and sufficient internal and prospective validation confirmed the reliability and robustness of our results. Furthermore, its value in clinical practice as a tool to potentially guide personalized treatment is advantageous. This non-invasive model calculated the possibility of each patient reaching ypT0-2 stage, which could play a role in making organ-preservation decisions. Additionally, the model could help select potential patients suitable for adequate consolidation chemotherapy treatment, which increased the clinical value of this model.

This study had some limitations. First, we included no specific therapeutic schedules for consolidation chemotherapy other than chemotherapy cycles. Few patients had adequate consolidation chemotherapy. In

our prospective cohort, only four patients had completed adequate consolidation chemotherapy, of whom three reached ypT0-2. Adequate consolidation chemotherapy benefits should be assessed in a larger, detailed cohort. Second, the delineation of ROI in the present study was manually conducted by one operator and verified by an expert. It could be more promising if two operators did the delineation and calculated intraclass correlation coefficient to verify the stability. Third, only T2WI sequences were used to extract radiomic features, since T2WI is the recommended MRI sequence (61) and suitable for each patient. Additionally, T2WI sequences based radiomics was used to predict pathologic T stage (62), perineural invasion (63), and pathological complete response (64-66) in rectal cancer, suggesting its promising prediction performance. Given the parameter heterogeneity of other sequences and good T2WI sequence consistency in each centre, despite less radiomic information, this single MRI sequence-based model could be applied in robustness to other medical centres.

5. Conclusions

In conclusion, we identified and validated a multicentre, pre-treatment MRI-based model for predicting ypT0-2 in patients with LARC. This model may facilitate personalized treatment decision-making for organ-preservation strategies and consolidation chemotherapy.

Acknowledgments

We would like to thank Editage (www.editage.cn) for English language editing.

Authors' Contributions

WW and HT participated in study design and paper draft revision. YX, SL, and HW participated in statistical analysis and drafted the manuscript. MS, KH, FW, YC, YL, XZ, JG, and YZ participated in data acquisition or ROI delineation. YX, ZW, ZN, and JL participated in technical and statistical support. All the authors approved the final draft for submission.

Declarations of Interest

None.

Fundings

This work was supported by the Beijing Hospitals Authority's Ascent Plan (grand number DFL 20220902), the Beijing Municipal Science & Technology Commission (grand number Z181100001718192), Science Foundation of Peking University Cancer Hospital (grand number 18-03), Beijing Natural Science Foundation (grand number 7182028), Clinical Technology Innovation Project of Beijing Hospital Authority (grand number XMLX201842), Capital's Funds for Health Improvement and Research (grand numbers 2020-2-1027, 2020-1-4021), and National Natural Science Foundation (grand number 82073333, 32071156).

References

1. Kapiteijn E, Marijnen CA, Nagtegaal ID, Putter H, Steup WH, Wiggers T, et al. Preoperative radiotherapy combined with total mesorectal excision for resectable rectal cancer. N Engl J Med. 2001;345(9):638-46.

2. Bryant CL, Lunniss PJ, Knowles CH, Thaha MA, Chan CL. Anterior resection syndrome. Lancet Oncol. 2012;13(9):e403-8.

3. Thaysen HV, Jess P, Rasmussen PC, Nielsen MB, Laurberg S. Health-related quality of life after surgery for advanced and recurrent rectal cancer: a nationwide prospective study. Colorectal Dis. 2014;16(7):O223-33.

4. Sajid MS, Farag S, Leung P, Sains P, Miles WF, Baig MK. Systematic review and meta-analysis of published trials comparing the effectiveness of transanal endoscopic microsurgery and radical resection in the management of early rectal cancer. Colorectal Dis. 2014;16(1):2-14.

5. Chiloiro G, Meldolesi E, Giraffa M, Capocchiano ND, Barbaro B, Coco C, et al. Could the conservative approach be considered safe in the treatment of locally advanced rectal cancer in case of a clinical near-complete or complete response? A retrospective analysis. Clin Transl Radiat Oncol. 2021;28:1-9.

6. Creavin B, Ryan E, Martin ST, Hanly A, O'Connell PR, Sheahan K, et al. Organ preservation with local excision or active surveillance following chemoradiotherapy for rectal cancer. Br J Cancer. 2017;116(2):169-74.

7. Stijns RCH, de Graaf EJR, Punt CJA, Nagtegaal ID, Nuyttens J, van Meerten E, et al. Long-term Oncological and Functional Outcomes of Chemoradiotherapy Followed by Organ-Sparing Transanal Endoscopic Microsurgery for Distal Rectal Cancer: The CARTS Study. JAMA Surg. 2019;154(1):47-54.

8. Xiong X, Wang C, Wang B, Shen Z, Jiang K, Gao Z, et al. Can transanal endoscopic microsurgery effectively treat T1 or T2 rectal cancer?A systematic review and meta-analysis. Surg Oncol. 2021;37:101561.

9. Ahmad NZ, Abbas MH, Abunada MH, Parvaiz A. A Meta-analysis of Transanal Endoscopic Microsurgery versus Total Mesorectal Excision in the Treatment of Rectal Cancer. Surg J (N Y). 2021;7(3):e241-e50.

10. Perez RO, Habr-Gama A, Sao Juliao GP, Proscurshim I, Fernandez LM, de Azevedo RU, et al. Transanal Endoscopic Microsurgery (TEM) Following Neoadjuvant Chemoradiation for Rectal Cancer: Outcomes of Salvage Resection for Local Recurrence. Ann Surg Oncol. 2016;23(4):1143-8.

11. Garcia-Aguilar J, Chow OS, Smith DD, Marcet JE, Cataldo PA, Varma MG, et al. Effect of adding mFOLFOX6 after neoadjuvant chemoradiation in locally advanced rectal cancer: a multicentre, phase 2 trial. Lancet Oncol. 2015;16(8):957-66.

12. Fokas E, Allgauer M, Polat B, Klautke G, Grabenbauer GG, Fietkau R, et al. Randomized Phase II Trial of Chemoradiotherapy Plus Induction or Consolidation Chemotherapy as Total Neoadjuvant Therapy for Locally Advanced Rectal Cancer: CAO/ARO/AIO-12. J Clin Oncol. 2019;37(34):3212-22.

13. Kim SY, Joo J, Kim TW, Hong YS, Kim JE, Hwang IG, et al. A Randomized Phase 2 Trial of Consolidation Chemotherapy After Preoperative Chemoradiation Therapy Versus Chemoradiation Therapy Alone for Locally Advanced Rectal Cancer: KCSG CO 14-03. Int J Radiat Oncol Biol Phys. 2018;101(4):889-99.

14. Patel UB, Brown G, Machado I, Santos-Cores J, Pericay C, Ballesteros E, et al. MRI assessment and outcomes in patients receiving neoadjuvant chemotherapy only for primary rectal cancer: long-term results from the GEMCAD 0801 trial. Ann Oncol. 2017;28(2):344-53.

15. Liu Z, Meng X, Zhang H, Li Z, Liu J, Sun K, et al. Predicting distant metastasis and chemotherapy benefit in locally advanced rectal cancer. Nat Commun. 2020;11(1):4308.

16. Bulens P, Couwenberg A, Intven M, Debucquoy A, Vandecaveye V, Van Cutsem E, et al. Predicting the tumor response to chemoradiotherapy for rectal cancer: Model development and external validation using MRI radiomics. Radiother Oncol. 2020;142:246-52.

17. Delli Pizzi A, Chiarelli AM, Chiacchiaretta P, d'Annibale M, Croce P, Rosa C, et al. MRI-based clinical-radiomics model predicts tumor response before treatment in locally advanced rectal cancer. Sci Rep. 2021;11(1):5379.

18. Li JL, Ji JF, Cai Y, Li XF, Li YH, Wu H, et al. Preoperative concomitant boost intensity-modulated radiotherapy with oral capecitabine in locally advanced mid-low rectal cancer: a phase II trial. Radiother Oncol. 2012;102(1):4-9.

19. Lee LC, Liong CY, Jemain AA. Partial least squares-discriminant analysis (PLS-DA) for classification of high-dimensional (HD) data: a review of contemporary practice strategies and knowledge gaps. Analyst. 2018;143(15):3526-39.

20. Song M, Li S, Wang H, Hu K, Wang F, Teng H, et al. MRI radiomics independent of clinical baseline characteristics and neoadjuvant treatment modalities predicts response to neoadjuvant therapy in rectal cancer. Br J Cancer. 2022.

21. Wang XH, Long LH, Cui Y, Jia AY, Zhu XG, Wang HZ, et al. MRI-based radiomics model for preoperative prediction of 5-year survival in patients with hepatocellular carcinoma. Br J Cancer. 2020;122(7):978-85.

22. Luna-Perez P, Rodriguez-Ramirez S, Vega J, Sandoval E, Labastida S. Morbidity and mortality following abdominoperineal resection for low rectal adenocarcinoma. Rev Invest Clin. 2001;53(5):388-

95.

23. Baxter NN, Garcia-Aguilar J. Organ preservation for rectal cancer. J Clin Oncol. 2007;25(8):1014-20.

24. Habr-Gama A, Perez RO, Nadalin W, Sabbaga J, Ribeiro U, Jr., Silva e Sousa AH, Jr., et al. Operative versus nonoperative treatment for stage 0 distal rectal cancer following chemoradiation therapy: long-term results. Ann Surg. 2004;240(4):711-7; discussion 7-8.

25. Habr-Gama A, Gama-Rodrigues J, Sao Juliao GP, Proscurshim I, Sabbagh C, Lynn PB, et al. Local recurrence after complete clinical response and watch and wait in rectal cancer after neoadjuvant chemoradiation: impact of salvage therapy on local disease control. Int J Radiat Oncol Biol Phys. 2014;88(4):822-8.

26. Maas M, Nelemans PJ, Valentini V, Das P, Rodel C, Kuo LJ, et al. Long-term outcome in patients with a pathological complete response after chemoradiation for rectal cancer: a pooled analysis of individual patient data. Lancet Oncol. 2010;11(9):835-44.

27. Moon SH, Kim DY, Park JW, Oh JH, Chang HJ, Kim SY, et al. Can the new American Joint Committee on Cancer staging system predict survival in rectal cancer patients treated with curative surgery following preoperative chemoradiotherapy? Cancer. 2012;118(20):4961-8.

28. Shaikh I, Askari A, Ouru S, Warusavitarne J, Athanasiou T, Faiz O. Oncological outcomes of local excision compared with radical surgery after neoadjuvant chemoradiotherapy for rectal cancer: a systematic review and meta-analysis. Int J Colorectal Dis. 2015;30(1):19-29.

29. Van den Eynde F, Jaekers J, Fieuws S, D'Hoore AM, Wolthuis AM. TAMIS is a valuable alternative to TEM for resection of intraluminal rectal tumors. Tech Coloproctol. 2019;23(2):161-6.

30. Stipa F, Tierno SM, Russo G, Burza A. Trans-anal minimally invasive surgery (TAMIS) versus

trans-anal endoscopic microsurgery (TEM): a comparative case-control matched-pairs analysis. Surg Endosc. 2022;36(3):2081-6.

31. Chaouch MA, Khan J, Gill TS, Mehrabi A, Reissfelder C, Rahberi N, et al. Early salvage total mesorectal excision (sTME) after organ preservation failure in rectal cancer does not worsen postoperative outcomes compared to primary TME: systematic review and meta-analysis. Int J Colorectal Dis. 2021;36(11):2375-86.

32. Levic Souzani K, Bulut O, Kuhlmann TP, Gogenur I, Bisgaard T. Completion total mesorectal excision following transanal endoscopic microsurgery does not compromise outcomes in patients with rectal cancer. Surg Endosc. 2022;36(2):1181-90.

33. Rullier E, Rouanet P, Tuech JJ, Valverde A, Lelong B, Rivoire M, et al. Organ preservation for rectal cancer (GRECCAR 2): a prospective, randomised, open-label, multicentre, phase 3 trial. Lancet. 2017;390(10093):469-79.

34. Fernandez LM, Figueiredo NL, Habr-Gama A, Sao Juliao GP, Vieira P, Vailati BB, et al. Salvage Surgery With Organ Preservation for Patients With Local Regrowth After Watch and Wait: Is It Still Possible? Dis Colon Rectum. 2020;63(8):1053-62.

35. Zhou X, Yi Y, Liu Z, Zhou Z, Lai B, Sun K, et al. Radiomics-Based Preoperative Prediction of Lymph Node Status Following Neoadjuvant Therapy in Locally Advanced Rectal Cancer. Front Oncol. 2020;10:604.

36. Kim MJ, Hur BY, Lee ES, Park B, Joo J, Kim MJ, et al. Prediction of lateral pelvic lymph node metastasis in patients with locally advanced rectal cancer with preoperative chemoradiotherapy: Focus on MR imaging findings. PLoS One. 2018;13(4):e0195815.

37. Zhu H, Zhang X, Li X, Shi Y, Zhu H, Sun Y. Prediction of pathological nodal stage of locally

advanced rectal cancer by collective features of multiple lymph nodes in magnetic resonance images before and after neoadjuvant chemoradiotherapy. Chin J Cancer Res. 2019;31(6):984-92.

38. Pomerri F, Crimi F, Veronese N, Perin A, Lacognata C, Bergamo F, et al. Prediction of N0 Irradiated Rectal Cancer Comparing MRI Before and After Preoperative Chemoradiotherapy. Dis Colon Rectum. 2017;60(11):1184-91.

39. Ma X, Shen F, Jia Y, Xia Y, Li Q, Lu J. MRI-based radiomics of rectal cancer: preoperative assessment of the pathological features. BMC Med Imaging. 2019;19(1):86.

40. Duchalais E, Glyn Mullaney T, Spears GM, Kelley SR, Mathis K, Harmsen WS, et al. Prognostic value of pathological node status after neoadjuvant radiotherapy for rectal cancer. Br J Surg. 2018;105(11):1501-9.

41. Kim DW, Kim DY, Kim TH, Jung KH, Chang HJ, Sohn DK, et al. Is T classification still correlated with lymph node status after preoperative chemoradiotherapy for rectal cancer? Cancer. 2006;106(8):1694-700.

42. Dumont F, Dartigues P, Delga B, Thibaudeau E, Benhaim L, Campion L, et al. Model predicting the ypN0 status after good response to chemoradiotherapy in rectal cancer. Am J Surg. 2018;216(3):438-43.

43. Wang D, Xu J, Zhang Z, Li S, Zhang X, Zhou Y, et al. Evaluation of Rectal Cancer Circumferential Resection Margin Using Faster Region-Based Convolutional Neural Network in High-Resolution Magnetic Resonance Images. Dis Colon Rectum. 2020;63(2):143-51.

44. Liu H, Zhang C, Wang L, Luo R, Li J, Zheng H, et al. MRI radiomics analysis for predicting preoperative synchronous distant metastasis in patients with rectal cancer. Eur Radiol. 2019;29(8):4418-26.

45. Nie K, Shi L, Chen Q, Hu X, Jabbour SK, Yue N, et al. Rectal Cancer: Assessment of Neoadjuvant Chemoradiation Outcome based on Radiomics of Multiparametric MRI. Clin Cancer Res. 2016;22(21):5256-64.

46. Liu Z, Zhang XY, Shi YJ, Wang L, Zhu HT, Tang Z, et al. Radiomics Analysis for Evaluation of Pathological Complete Response to Neoadjuvant Chemoradiotherapy in Locally Advanced Rectal Cancer. Clin Cancer Res. 2017;23(23):7253-62.

47. Zhang XY, Wang L, Zhu HT, Li ZW, Ye M, Li XT, et al. Predicting Rectal Cancer Response to Neoadjuvant Chemoradiotherapy Using Deep Learning of Diffusion Kurtosis MRI. Radiology. 2020;296(1):56-64.

48. Shayesteh S, Nazari M, Salahshour A, Sandoughdaran S, Hajianfar G, Khateri M, et al. Treatment response prediction using MRI-based pre-, post-, and delta-radiomic features and machine learning algorithms in colorectal cancer. Med Phys. 2021;48(7):3691-701.

49. Wan L, Peng W, Zou S, Ye F, Geng Y, Ouyang H, et al. MRI-based delta-radiomics are predictive of pathological complete response after neoadjuvant chemoradiotherapy in locally advanced rectal cancer. Acad Radiol. 2021;28 Suppl 1:S95-S104.

50. Jeon SH, Song C, Chie EK, Kim B, Kim YH, Chang W, et al. Delta-radiomics signature predicts treatment outcomes after preoperative chemoradiotherapy and surgery in rectal cancer. Radiat Oncol. 2019;14(1):43.

51. Chiloiro G, Rodriguez-Carnero P, Lenkowicz J, Casa C, Masciocchi C, Boldrini L, et al. Delta Radiomics Can Predict Distant Metastasis in Locally Advanced Rectal Cancer: The Challenge to Personalize the Cure. Front Oncol. 2020;10:595012.

52. Boldrini L, Cusumano D, Chiloiro G, Casa C, Masciocchi C, Lenkowicz J, et al. Delta radiomics for

rectal cancer response prediction with hybrid 0.35 T magnetic resonance-guided radiotherapy (MRgRT): a hypothesis-generating study for an innovative personalized medicine approach. Radiol Med. 2019;124(2):145-53.

53. Nardone V, Reginelli A, Grassi R, Vacca G, Giacobbe G, Angrisani A, et al. Ability of Delta Radiomics to Predict a Complete Pathological Response in Patients with Loco-Regional Rectal Cancer Addressed to Neoadjuvant Chemo-Radiation and Surgery. Cancers (Basel). 2022;14(12).

54. Zhao S, Chen X, Wen D, Zhang C, Wang X. Oncologic Nomogram for Stage I Rectal Cancer to Assist Patient Selection for Adjuvant (Chemo)Radiotherapy Following Local Excision. Front Oncol. 2021;11:632085.

55. Hong Y, Ghuman A, Poh KS, Krizzuk D, Nagarajan A, Amarnath S, et al. Can normalized carcinoembryonic antigen following neoadjuvant chemoradiation predict tumour recurrence after curative resection for locally advanced rectal cancer? Colorectal Dis. 2021;23(6):1346-56.

56. Pang X, Gao Y, Yi H, Liu H, Liu S, Zheng J. Associations between clinical characteristics and tumor response to neoadjuvant chemoradiotherapy in rectal cancer. Cancer Med. 2021;10(14):4832-43.

57. Mbanu P, Osorio EV, Mistry H, Malcomson L, Yousif S, Aznar M, et al. Clinico-pathological predictors of clinical complete response in rectal cancer. Cancer Treat Res Commun. 2022;31:100540.

58. Patel SV, Roxburgh CS, Vakiani E, Shia J, Smith JJ, Temple LK, et al. Distance to the anal verge is associated with pathologic complete response to neoadjuvant therapy in locally advanced rectal cancer. J Surg Oncol. 2016;114(5):637-41.

59. Restivo A, Zorcolo L, Cocco IM, Manunza R, Margiani C, Marongiu L, et al. Elevated CEA levels and low distance of the tumor from the anal verge are predictors of incomplete response to chemoradiation in patients with rectal cancer. Ann Surg Oncol. 2013;20(3):864-71.

60. Moore J, Price T, Carruthers S, Selva-Nayagam S, Luck A, Thomas M, et al. Prospective randomized trial of neoadjuvant chemotherapy during the 'wait period' following preoperative chemoradiotherapy for rectal cancer: results of the WAIT trial. Colorectal Dis. 2017;19(11):973-9.

61. Beets-Tan RGH, Lambregts DMJ, Maas M, Bipat S, Barbaro B, Curvo-Semedo L, et al. Magnetic resonance imaging for clinical management of rectal cancer: Updated recommendations from the 2016 European Society of Gastrointestinal and Abdominal Radiology (ESGAR) consensus meeting. Eur Radiol. 2018;28(4):1465-75.

62. Sun Y, Hu P, Wang J, Shen L, Xia F, Qing G, et al. Radiomic features of pretreatment MRI could identify T stage in patients with rectal cancer: Preliminary findings. J Magn Reson Imaging. 2018.

63. Guo Y, Wang Q, Guo Y, Zhang Y, Fu Y, Zhang H. Preoperative prediction of perineural invasion with multi-modality radiomics in rectal cancer. Sci Rep. 2021;11(1):9429.

64. Meng Y, Zhang C, Zou S, Zhao X, Xu K, Zhang H, et al. MRI texture analysis in predicting treatment response to neoadjuvant chemoradiotherapy in rectal cancer. Oncotarget. 2018;9(15):11999-2008.

65. Aker M, Ganeshan B, Afaq A, Wan S, Groves AM, Arulampalam T. Magnetic Resonance Texture Analysis in Identifying Complete Pathological Response to Neoadjuvant Treatment in Locally Advanced Rectal Cancer. Dis Colon Rectum. 2019;62(2):163-70.

66. De Cecco CN, Ganeshan B, Ciolina M, Rengo M, Meinel FG, Musio D, et al. Texture analysis as imaging biomarker of tumoral response to neoadjuvant chemoradiotherapy in rectal cancer patients studied with 3-T magnetic resonance. Invest Radiol. 2015;50(4):239-45.

Conflicts of interest

None.

Highlights

- Pre-treatment MRI images were used to construct a prediction model for pathologic T downstaging in locally advanced rectal cancer.
- The prediction model showed good performance in training cohort (AUC 0.842) , internal testing cohort (AUC 0.809) and prospective cohort (AUC 0.727).
- High-probability group (score>81.82) had potential benefits from sufficient consolidation chemotherapy.